

Study of the influence of indium segregation on the optical properties of InGaAs/GaAs quantum wells via split-operator method

S. Martini^{a)}

Grupo de Pesquisa em Microeletrônica e Dispositivos Optoeletrônicos, Faculdade de Tecnologia e Ciências Exatas da Universidade São Judas Tadeu, São Paulo, SP 03166-000, Brazil

J. E. Manzoli^{b)}

Grupo de Pesquisa em Microeletrônica e Dispositivos Optoeletrônicos, Faculdade de Tecnologia e Ciências Exatas da Universidade São Judas Tadeu, São Paulo, SP 03166-000, Brazil and Instituto de Pesquisas Energéticas e Nucleares (IPEN), Centro de Tecnologia das Radiações (CTR), São Paulo, SP 05508-000, Brazil

A. A. Quivy

Laboratório de Novos Materiais Semicondutores, Instituto de Física da Universidade de São Paulo, CP 66318, São Paulo, SP 05315-970, Brazil

(Received 22 July 2009; accepted 4 January 2010; published 19 March 2010)

In the case of quantum wells, the indium segregation leads to complex potential profiles that are hardly considered in the majority of the theoretical models. The authors demonstrated that the split-operator method is useful tool for obtaining the electronic properties in these cases. Particularly, they studied the influence of the indium surface segregation in optical properties of InGaAs/GaAs quantum wells. Photoluminescence measurements were carried out for a set of InGaAs/GaAs quantum wells and compared to the results obtained theoretically via split-operator method, showing a good agreement. © 2010 American Vacuum Society. [DOI: 10.1116/1.3301612]

I. INTRODUCTION

The growth of strained $\text{In}_x\text{Ga}_{1-x}\text{As}/\text{GaAs}$ quantum wells (QWs) of high quality is very important to the micro- and optoelectronic industries since these wells can be used in a large range of high-performance devices, such as high-mobility transistors and strained-layer lasers operating in the 980 nm region.^{1,2} For most of these applications, the In fraction, x , must be less than 0.25 in order to achieve a sufficiently thick strained layer without any structural defects. However, it is now also well established that the heteroepitaxy of InGaAs layers on GaAs substrates is characterized by a strong segregation of indium (In) atoms that accumulate at the growth front and strongly modify the In-composition profile, resulting in different electronic and optical properties of the devices based on that material.

Due to its fundamental importance, during the past decades remarkable progress has been achieved on the understanding of the segregation process. These studies treat, among many aspects, the different techniques of characterization to identify the segregation, as well as some solutions during the growth for reducing the problem. The first work to show the trend of indium segregation during the molecular beam epitaxy (MBE) growth of III-V compounds appeared in literature in 1987 with the results of Massies *et al.*³ In 1989, Moison *et al.*⁴ held a first systematic study of segregation of atoms of column IIIA, showing that the segregation of indium is much greater than that of aluminum and gallium and following the order: $\text{In} > \text{Al} > \text{Ga}$. In 1992, Gerard and

Marzin,⁵ investigating $\text{InAs}/\text{GaAs}/\text{Ga}_{1-y}\text{Al}_y\text{As}$ QWs, obtained by photoluminescence (PL) the indium composition profile in the interface of the quantum wells.

In the same year, Muraki *et al.*,⁶ in a pioneering work, showed the influence of indium segregation on the energy levels of $\text{In}_x\text{Ga}_{1-x}\text{As}/\text{GaAs}$ QWs. By using the technique of PL and secondary ion mass spectroscopy (SIMS), the authors carried out a systematic study of indium segregation under various growth conditions. Through a phenomenological model, Muraki *et al.*⁶ assumed that a fraction R (denoted as the segregation coefficient) of the In atoms in the last epitaxial layer always segregates to the surface layer during the growth of each new layer, whereas the portion $(1-R)$ remains incorporated in the crystal.

In the following year, 1993, Nagle *et al.*,⁷ using the techniques of ultraviolet of photoelectron spectroscopy (UPS) and reflection high-energy electron diffraction (RHEED), determined the indium surface segregation under different growth conditions, including, in addition to the growth temperature, the ratio between the flows of III-V elements. This was the first work that showed that the indium segregation was sensitive to the III/V ratio.

This was followed by three other works that deserve attention. The first is the work of Zheng *et al.*,⁸ published in 1994, that by using a tunneling electron microscope (TEM), they could observe, for the first time at the atomic level, the roughness of the interfaces of $\text{In}_x\text{Ga}_{1-x}\text{As}/\text{GaAs}$ QWs due to the indium segregation. The results of that study show that the interface of GaAs on $\text{In}_{0.2}\text{Ga}_{0.8}\text{As}$ is thicker around five to ten atomic layers, while the interface of $\text{In}_{0.2}\text{Ga}_{0.8}\text{As}$ on GaAs is about two to four layers wider than the ideal profile. The second work, published in 1995 by Yu *et al.*⁹

^{a)}Electronic mail: prof.martini@gmail.com

^{b)}Electronic mail: jmanzoli@ipen.br

showed that the segregation of indium could lead to the formation of islands located above the interfaces and, consequently, cause the emergence of additional transitions in the PL spectrum. Finally, in 2002, Martini *et al.*¹⁰ proposed a simple and very effective way to determine, *in situ* and in real time, the In segregation atoms during the growth of InGaAs layers on GaAs. The method is based on an interpretation of the intensity variation in the RHEED oscillations and allows a direct determination of the segregation coefficient R introduced by Muraki *et al.*⁶

However, a number of other experimental works were also published concomitant with the works cited above. All these works proposed characterization techniques to determine the indium surface segregation. Among the variety of techniques, some used *in situ* techniques that include UPS,^{4,7,11} RHEED,^{5,12} reflection mass spectrometry,¹³ difference-reflectance spectroscopy,¹⁴ and x-ray photoelectron spectroscopy^{4,15} and *ex situ* techniques including PL,^{5,6,16} SIMS,^{6,17} TEM,^{18–20} x-ray,^{21,22} electrolyte electroreflectance,²³ and optical thermally detected optical absorption.²⁴ In each of these techniques, within their characteristics, a significant widening of the interface In_xGa_{1-x}As/GaAs was observed and attributed to the indium segregation during growth. Besides the already well In segregation on arsenides alloys, it was also observed antimony segregation at the arsenide-on-antimonide interface, indium segregation at the antimonide-on-arsenide interface for InAs/GaSb multiple quantum wells,²⁵ and Sb segregation in GaInSb/InAs strained-layer superlattices.²⁶

In spite of a considerable number of experimental works, there is a lack of theoretical ones, mainly due to the difficulty in properly simulating the real profile of the potential under the effect of the indium segregation. To our knowledge, there are two theoretical works that simulate the influence of indium segregation on the energy levels in the InGaAs/GaAs QWs, considering different potential profiles and widths. The first one, by de la Cruz,²⁷ consider a smooth symmetrical potential, which does not correspond to the real profile. The second, by Schowalter *et al.*,²⁸ by considering an eight-band Kane model, obtained the behavior of the energetic position of the PL peak intensities as a function of the segregation efficiency R , the concentration x_0 , and the QW thickness. However, neither work considered the exciton energies. Further comparison with experimental results is needed. Therefore, a systematic and rigorous study of the influence of indium segregation on the electronic levels and optical properties in InGaAs/GaAs QWs considering the real potential profile, as well as the exciton energies, in which quantitative results can be obtained and compared directly with experiments, is of great importance.

In this work, by considering the split-operator method (SOM),^{29–31} we study the influence of the indium segregation on the confined electron/hole states of the InGaAs/GaAs QWs and compare that with experimental results obtained by PL. This article is organized as follows. In Sec. II, we describe the experimental details. In Sec. III, we show the the-

oretical approach. In Sec. IV, we made a comparison with experimental data. Finally, Sec. V is devoted to the conclusions.

II. EXPERIMENT

The sample investigated here was grown in a Mod Gen II MBE system from Varian. The sample consisted of 12 500-Å-thick GaAs buffer layer grown at 600 °C. The complete structure consisted of five In_{0.16}Ga_{0.84}As QWs of different nominal thickness (63, 51, 39, 27, and 15 Å) grown at 530 °C and surrounded by 500-Å-thick GaAs barriers grown at 600 °C. In the same sample, there are three GaAs QWs of different nominal thickness (150, 70, and 35 Å) grown at 580 °C and surrounded by 500-Å-thick Al_{0.35}Ga_{0.65}As barriers grown at 587 °C. The PL spectra were recorded by lock-in techniques. The samples were excited by the 5145 Å line of an Ar⁺ laser, the beam of which could be focused into the sample with a diameter of 100 μm. The measurements were carried out in an optical helium-bath cryostat operating with a microvalve and a helium pump in order to achieve the temperature of 1.4 K in the sample.

III. CALCULATION METHODS

A. Muraki's segregation model

The first segregation model for compound semiconductors was proposed by Moison *et al.*⁴ and was based on the exchange of atoms between the surface layer (constituted of physisorbed species with a large surface mobility) and the topmost crystalline epitaxial layer (bulk layer). In the case of InGaAs deposition on top of a GaAs substrate, a Ga adatom adsorbed on the surface would substitute an In atom already incorporated in the top epitaxial layer, leading to the segregation of an In atom from the bulk layer to the surface layer. However, the model predicts that segregation should decrease with increasing temperature, unlike what actually happens in these systems.

A few years later, Muraki *et al.*⁶ proposed a phenomenological model, based on SIMS and PL results, where a fraction R , named segregation coefficient, of the In atoms in the last epitaxial layer always segregates to the surface layer during the growth of each new layer. The remaining fraction $(1-R)$ of In atoms is incorporated in the crystal and the composition of indium in the n th layer is given by

$$x_{\text{bulk}}^{\text{In}}(n) = \begin{cases} x_0(1 - R^n) & (1 \leq n \leq N) \\ x_0(1 - R^N)R^{n-N} & (n > N), \end{cases} \quad (1)$$

with N as the number of InGaAs layers grown before depositing GaAs on top of the InGaAs material and x_0 as the nominal In content. Therefore, the In content at the surface is given by

$$x_{\text{surface}}^{\text{In}}(n+1) = \frac{R}{1-R} x_{\text{bulk}}^{\text{In}}(n). \quad (2)$$

Figure 1 shows schematically Muraki's model as described by the equations above. It is important to emphasize that Eq. (2) of Muraki and the model of Moison clearly predict the

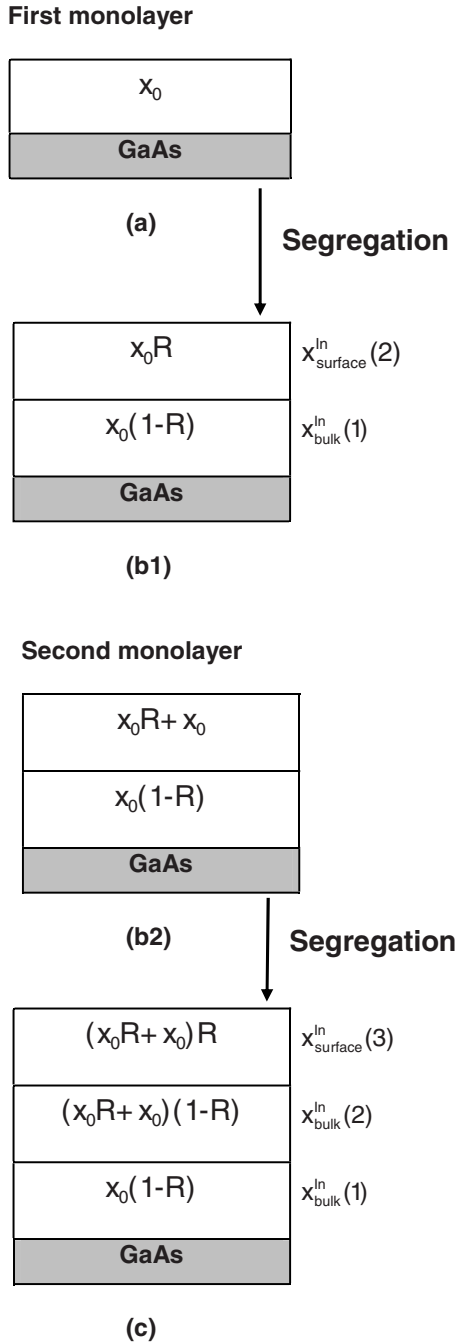


FIG. 1. Evolution of the indium concentration according to Muraki's model. Each box corresponds 1 ML (monolayer). In case (a) the first monolayer of $\text{In}_{x_0}\text{Ga}_{1-x_0}\text{As}$ is deposited with a nominal indium composition x_0 . Due to the segregation effects only a portion $(1-R)$ of indium atoms is incorporated and the rest R segregate to surface as shown in (b1). In the next step (b2), the second monolayer with a nominal indium composition x_0 is deposited. Consequently this monolayer will have an indium composition that will be $x_0 R + x_0$, but again due to the segregation effect, a portion $(1-R)$ of indium atoms is incorporated and the rest segregate to the surface (c).

segregation of part of the In atoms from the bulk layer to the surface of the sample. Until lately little was known about the chemical state of those atoms: Were they adsorbed on the surface and mobile or incorporated into a crystalline InAs layer? Recently, García *et al.*³² gave the answer in a very elegant experiment where the strain of the epitaxial layer was

measured *in situ* during the MBE growth of InAs on a GaAs substrate. They could only measure part of the strain that was expected if all the incoming In atoms were incorporated as InAs, meaning that a fraction of the In atoms was not present in that InAs crystalline layer and was most probably adsorbed on the surface. When a GaAs cap layer was grown on top of the InAs material, an extra strain was further detected and quantitatively related to the gradual incorporation of the floating In fraction during the GaAs growth. This experiment shows, without any doubt, that during the deposition of InGaAs, part of the incident In atoms does not incorporate into the crystal and is actually adsorbed on the surface (i.e., does not contribute to the growth). A second important consequence is that In segregation can occur without the presence of any incident Ga flux (in García's experiment, only InAs was deposited, not InGaAs), indicating that the phenomenon seems to be mainly strain driven. This was recently confirmed by Rosenauer *et al.*,³³ who showed (using careful TEM experiments) that although the Muraki model is purely phenomenological, it is in total agreement with all these new experimental results because it only concerns In atoms (and does not consider the Ga species).

In this work, we use Muraki's model to determine the influence of the indium segregation. Figure 2 depicts the In composition profile for three quantum wells with different widths, by considering two different segregation coefficient R according to Muraki's model. We observe that the segregation changes drastically the quantum well profile.

B. Split-operator method

By using Muraki's model to correctly describe the In concentration profiles, we derive potentials for electrons (ΔE_e) and heavy holes (ΔE_{hh}) and compute the electronic levels by numerically solving the Schrödinger equation via SOM for electrons (E_e) and heavy holes (E_{hh}) confined in the potential deduced from In concentration profiles. The great advantage of SOM is that any potential profile can be considered.

Now we focus our attention in describing briefly the SOM, in which the technique used to obtain the eigenvalues of the Schrödinger equation is based on the split-operator scheme²⁹ used previously by one of the present authors.^{34,35} It is considered that space and time are discretized in steps or finite differences. The method starts from the solution of the time-dependent Schrödinger equation for a slow-varying Hamiltonian, formally given by

$$\Psi(t + \Delta t) = e^{1/i\hbar \int_t^{t+\Delta t} H dt} \Psi(t) \cong e^{-iH\Delta t/\hbar} \Psi(t). \quad (3)$$

Then, the time evolution of the wave packet Ψ is obtained according to the procedure described by Degani,²⁹ where the Hamiltonian H is split into a kinetic operator K and a potential operator V ,

$$\begin{aligned} e^{-iH(\Delta t/\hbar)} &= e^{-i(\Delta t/\hbar)[K+V]} = e^{-i(\Delta t/\hbar)[V/2+K+V/2]} \\ &\cong e^{-i(\Delta t/\hbar)(V/2)} e^{-i(\Delta t/\hbar)K} e^{-i(\Delta t/\hbar)(V/2)} = \Gamma_1(x) e^{cK} \Gamma_1(x), \end{aligned} \quad (4)$$

where Γ_1 and c were used to simplify the mathematical no-

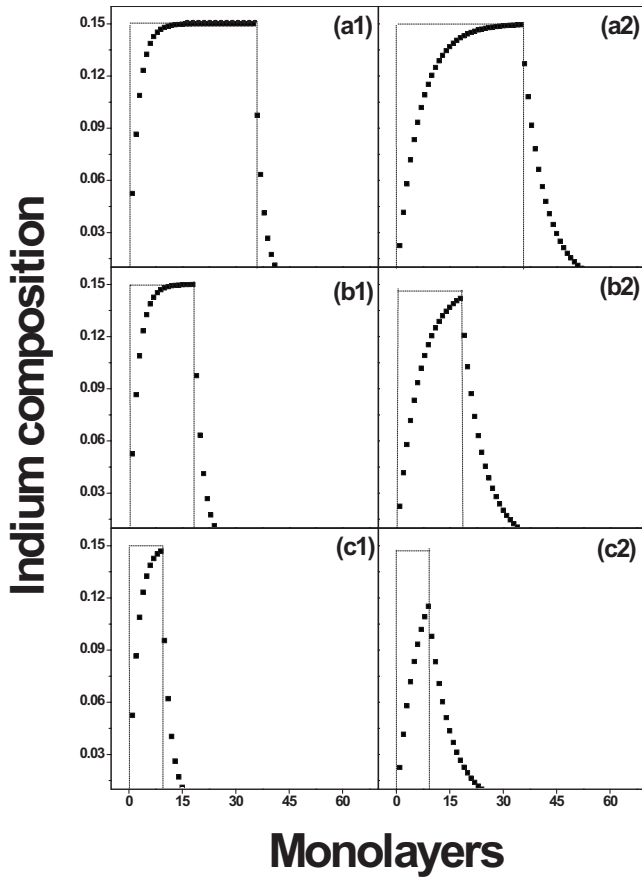


FIG. 2. Indium composition profile of $\text{In}_{0.15}\text{Ga}_{0.85}\text{As}$ QWs of (a) 100, (b) 50, and (c) 25 Å widths for segregation coefficient $R=0.65$ [labels (a1), (b1), and (c1)] and $R=0.85$ [labels (a2), (b2), and (c2)]. The dotted lines represent the ideal square QW profile ($R=0$). 1 ML is half of the InGaAs lattice parameter.

tation. Due to the noncommutativity of K and V , this is an approximation of order $(\Delta t)^3$.

In order to propagate the wave function in real space, the exponential is approximated as the unitary operator below,

$$e^{cK} \cong \frac{1 + cK/2}{1 - cK/2}, \quad (5)$$

which is correct up to $(\Delta t)^2$ order.

As shown in Eq. (3), in order to obtain the time evolution of the wave packet, we first operate Γ_1 on Ψ . Then, the operator described in Eq. (5) is applied on the resulting function.

If we call $(\Gamma_1\Psi)$ as (ξ) and $(e^{cK}\Gamma_1\Psi)$ as (η) , we have to solve the following equation:

$$(1 + cK/2)\xi = (1 - cK/2)\eta. \quad (6)$$

Writing Eq. (5) in the finite difference form in a nonuniform mesh,³⁶ the N points in which the function η was discretized, η_n , are the unknown variables of a tridiagonal nonhomogeneous linear system of equations. Once the system is solved and η is calculated, one computes $(\Gamma_1\eta)$ and gets the time evolution of Ψ .

Any wave packet is a linear combination of the eigenstates of the Hamiltonian and its time evolution is well described by the explained algorithm. This linear combination is expressed as

$$\Psi = \sum_j b_j(t)\varphi_j = \sum_j (a_j e^{-iE_j t/\hbar})\varphi_j, \quad (7)$$

where φ_j are the eigenstates.

Let us make a “numerical trick” calling the term it as τ . For the computer, if we consider τ as a real variable, the expression in Eq. (7) will result in a null function as time evolves. This is the same result if we propagate the wave packet in the split-operator algorithm: null function. However, if we oblige the wave packet to be normalized at each time step, this time evolution will be

$$\begin{aligned} \frac{\Psi}{\sqrt{\langle\Psi|\Psi\rangle}} &= \frac{\sum_{j=0} a_j \exp(-E_j \tau/\hbar) \varphi_j}{[\sum_{j=0} |a_j|^2 \exp(-2E_j \tau/\hbar)]^{1/2}} \\ &= \frac{(a_0/|a_0|)\varphi_0 + \sum_{j=1} (a_j/|a_0|)\exp(-(E_j - E_0)\tau/\hbar)\varphi_j}{[1 + \sum_{j=1} (|a_j|^2/|a_0|^2)\exp(-2(E_j - E_0)\tau/\hbar)]^{1/2}}. \end{aligned} \quad (8)$$

So, after a sufficient number of time steps, the “imaginary time” evolution of any wave packet will become the first eigenstate (ground state). This occurs because only the first term of the numerator of Eq. (8) does not become zero as time passes by. This is exactly what happens using the split-operator algorithm in imaginary time.

After obtained the ground state, we can get the second eigenstate doing the same imaginary evolution, but besides the normalization we have to oblige the orthogonalization of the wave packet with the ground state at each time step. The same should be made if we want the third, the fourth, etc., eigenstates, always obliging them to be orthonormalized with each other. Finally, the corresponding j eigenstate associated to each j eigenfunction is given by $\langle\varphi_j|H|\varphi_j\rangle$.

On a final note, we should observe that the temporal step is chosen in such a way as to assure fast convergence. As a general guideline, we followed a rule that is strictly valid only for linear parabolic partial equations with unitary coefficients and uniform discretization, but is useful here. It relates the time step and the spatial discretization interval of the finite-difference scheme by: $[\Delta\tau/(\Delta x_{\min})^2] \leq 0.5 \text{ fs}/\text{\AA}$.

C. Modeling the influence of the macroscopic strain

By using the algorithm described above, we considered an $\text{In}_{0.16}\text{Ga}_{0.84}\text{As}/\text{GaAs}$ QW and calculated the electron and heavy-hole confined states for different widths (15, 27, 39, 51, and 63 Å) and segregation coefficients $R=0$ (without the segregation effects, perfect square QWs) and $R=0.85$, which is a typical value for the growth conditions used here, as obtained by different experimental techniques.^{10,12,13,37} The structure and the indium composition were also chosen in order to compare with the experimental data. In order to determine the energy levels, we must consider the band offsets and the effective masses. In our case, we adopt for

TABLE I. Parameters used in our calculations. All were extracted from Ref. 42.

Parameters	GaAs	InAs
Lattice (Å)	5.65	6.08
a (eV)	-8.33	-6.08
b (eV)	-1.90	-1.55
C_{11} (Mbar)	1.22	0.83
C_{12} (Mbar)	0.57	0.45

the relative band offset for the valence 30% and for the conduction 70%, as usual. Concerning the effective masses, we considered the same masses used by Porto and Sánchez-Dehesa,³⁸ which already took into account the biaxial strain. The electron effective mass (m_e^*) and the heavy-hole effective mass (m_{hh}^*) as functions of In composition x

$$m_e^* = 0.067(1 - 0.426x)m_0,$$

$$m_{hh}^* = 0.34(1 + 0.117x)m_0, \quad (9)$$

where m_0 is the free electron mass. However, it is important to emphasize that we must also take into account the biaxial strain on the $\text{In}_x\text{Ga}_{1-x}\text{As}$ energy gap. The intrinsic strain present in the InGaAs layer comes from the difference in the lattice parameter between the ternary alloy and the GaAs buffer layer. The only way to impose biaxial stress to the epitaxial film is through matching of the lateral lattice parameter at the interface between both materials. The energy gap correction can be given by³⁹

$$\delta E_{hh} = 2a \left[\frac{C_{11} - C_{12}}{C_{11}} \right] \epsilon_{\parallel} - b \left[\frac{C_{11} + 2C_{12}}{C_{11}} \right] \epsilon_{\parallel}, \quad (10)$$

where a is the hydrostatic deformation potential, b is the deformation potential for tetragonal distortion, C_{11} and C_{12} are the elastic constants, and ϵ_{\parallel} is the strain given by

$$\epsilon_{\parallel} = \frac{a_{\text{GaAs}} - a_{\text{In}_x\text{Ga}_{1-x}\text{As}}}{a_{\text{In}_x\text{Ga}_{1-x}\text{As}}}, \quad (11)$$

where a_{GaAs} is the lattice parameter of the GaAs and $a_{\text{In}_x\text{Ga}_{1-x}\text{As}}$ is the lattice parameter of $\text{In}_x\text{Ga}_{1-x}\text{As}$ alloy. The values for the lattice parameter, deformation potentials, and elastic constants for GaAs and InAs are listed in Table I.

Therefore, the complete energy gap of $\text{In}_x\text{Ga}_{1-x}\text{As}$ layer is given by

$$E_g(\text{In}_x\text{Ga}_{1-x}\text{As}) = E_g(3D) + \delta E_{hh}, \quad (12)$$

where the energy gap of $\text{In}_x\text{Ga}_{1-x}\text{As}$ bulk as a function of indium composition, at 2 K, is given by⁴⁰

$$E_g(3D) = 1.5192 - 1.5837x + 0.475x^2 \text{ (eV)}. \quad (13)$$

In order to correctly compare the theoretical values with experimental PL data, the theoretical PL energy (E_{PL}) must be

$$E_{\text{PL}} = E_g(\text{In}_x\text{Ga}_{1-x}\text{As}) + E_e + E_{hh} - E_{\text{exc}}, \quad (14)$$

where E_{exc} is the binding energy of the heavy-hole exciton and was taken as 7 meV.⁴¹

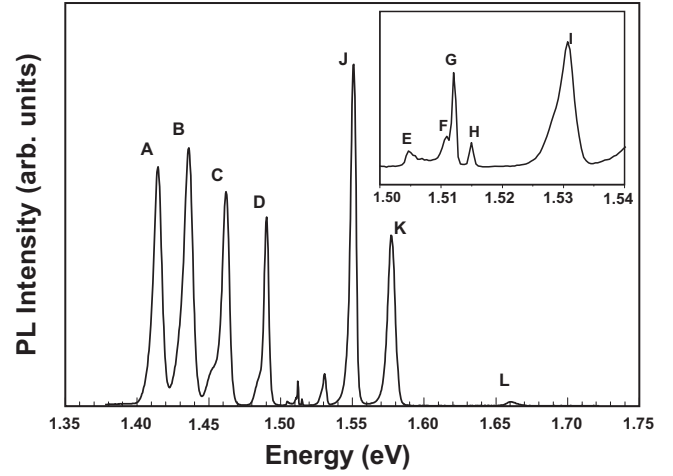


Fig. 3. PL spectrum at $T=1.4$ K and an excitation power of 30 mW. The inset shows in more detail the region between 1.50 and 1.54 eV. The peaks are labeled as described in the text.

IV. RESULTS AND DISCUSSION

Figure 3 depicts the PL spectrum for $T=1.4$ K and an excitation power of 30 mW. Each peak is identified by the corresponding excitonic transition energy. Peaks A, B, C, D, and E correspond to the excitonic transition energies between the ground states of electrons and heavy holes in the QWs of $\text{In}_{0.16}\text{Ga}_{0.84}\text{As}/\text{GaAs}$ of 63, 51, 39, 27, and 15 Å widths, respectively. The identifications of the observed peaks F (1.511 eV), G (1.512 eV), and H (1.515 eV) are as follows: (1) excitons bound to a Ga defect, (2) excitons bound to ionized donors, and (3) GaAs free exciton, respectively. The peaks J, K, and L correspond to the excitonic transition energies between the ground states of electrons and heavy holes in the QWs of $\text{Al}_{0.35}\text{Ga}_{0.65}\text{As}/\text{GaAs}$ of 150, 70, and 35 Å widths, respectively. Despite there being QWs of $\text{Al}_{0.35}\text{Ga}_{0.65}\text{As}/\text{GaAs}$ in this sample, we are only interested in the segregation effects on the emission originated from $\text{In}_{0.16}\text{Ga}_{0.84}\text{As}/\text{GaAs}$ QWs.

With the results obtained in Fig. 3, we obtained the behavior of the transition energies as a function of QW width for peaks A, B, C, D, and E, as depicted in Fig. 4. As already expected by basic quantum mechanics, the energy decreases with the QW width. However, the experimental energies are blueshifted in comparison with the predicted energies for an ideal square QW profile. This is a fingerprint of the In segregation effect, which has mainly two consequences. First, there is a remarkable change in the QW profile due to the indium segregation, as already shown in Fig. 2. This change is followed by a change in the energy levels of the QW. Second, if there is In segregation, we could expect an increase in the QW transition energy as a consequence of the lower In content in the layer that leads to a higher energy gap of the material. Thus it is very important to take into account the segregation effect in order to predict the optical behavior of InGaAs QWs correctly.

As mentioned before, the segregation coefficient R can be determined by RHEED measurements, as shown by Martini

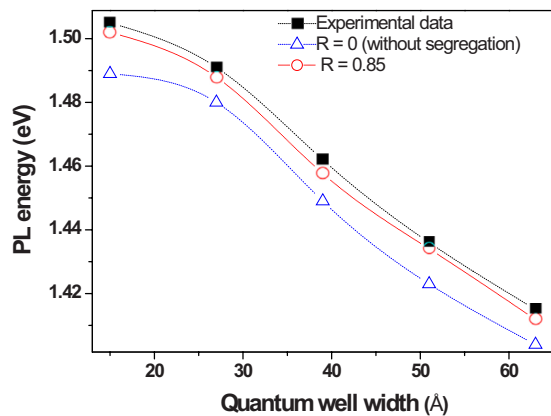


FIG. 4. (Color online) Transition energy of $\text{In}_{0.15}\text{Ga}_{0.85}\text{As}$ QWs as a function of the width. The full squares represent the experimental data, the open (blue) triangles represent the predicted energies of QWs without taking into account the segregation effect, and the open (red) circles correspond to the theoretical results taken into account by the segregation effect with $R=0.85$.

et al. in Ref. 10. By considering the results from RHEED measurements, when the InGaAs layers are deposited on GaAs surface, an asymmetric and strong damping can be observed. Since In segregation is strongly present in the InGaAs alloy and depends on those growth parameters in the same fashion, Martini *et al.*¹⁰ fitted the decay of the RHEED oscillations I in order to extract the In segregation by the expression

$$I = I_0 + I_1 \exp(-t/\lambda), \quad (15)$$

where I_0 and I_1 are constants, t is the growth time, and λ is the decay constant that is the relevant fitting parameter (t and λ can also be expressed in monolayers by simply multiplying them by the growth rate). The physical meaning of λ can be better understood when the segregation coefficient R introduced by Muraki *et al.*⁶ is written as

$$R = \exp(-1/\delta), \quad (16)$$

where δ is a characteristic length (expressed in monolayers) over which the effects of the segregation phenomenon can be effectively sensed. If we suppose that the damping of the InGaAs RHEED oscillations is related to In segregation, it should be possible to calculate R using λ (in monolayers) instead of δ in Eq. (16). Using the value of λ from the best fit of the experimental data, it was obtained $R=0.85$, which is a typical value for the growth conditions used here, as mentioned before.

For this value of R , we considered the segregation effects by considering the In composition profile according to Muraki's model within the split-operator method and obtained the transition energies. The results are also shown in Fig. 4. We can observe that the results now, with the segregation effects taken into account, have a much better agreement with the experimental data, showing that the segregation effects have a considerable contribution. Moreover, these effects can be correctly predicted by SOM. It is also worth

pointing out that the method was also applied for different In compositions, as well as growth temperatures, and also gave very good results.

V. CONCLUSIONS

In summary, in this work we analyze the influence of the indium surface segregation on the energy levels of the InGaAs/GaAs QWs by using SOM. We concluded that this method can simulate the real QWs profiles obtained from Muraki's model. We observed a very good agreement between the theoretical and experimental values. Hopefully, these studies on the indium segregation will stimulate other kind of theoretical investigations, allowing a more thorough understanding of these classic MBE issues.

ACKNOWLEDGMENTS

The authors would like to thank the Brazilian funding agencies, Fundação de Amparo Pesquisa do Estado de São Paulo (FAPESP), Conselho Nacional de Pesquisa (CNPq), and the research center of Universidade São Judas Tadeu for partial financial support. The authors also acknowledge Lara Kühl Teles for fruitful discussion.

- ¹M. Meshkinpour, M. S. Goorsky, B. Jenichen, D. C. Streit, and T. R. Block, *J. Appl. Phys.* **81**, 3124 (1997).
- ²M. C. Wu, N. A. Olsson, D. Sivco, and A. Y. Cho, *Appl. Phys. Lett.* **56**, 221 (1990).
- ³J. Massies, F. Turco, A. Salletes, and J. P. Contour, *J. Cryst. Growth* **80**, 307 (1987).
- ⁴J. M. Moison, C. Guille, F. Houzay, F. Barhte, and M. Van Rompay, *Phys. Rev. B* **40**, 6149 (1989).
- ⁵J.-M. Gerard and J.-Y. Marzin, *Phys. Rev. B* **45**, 6313 (1992).
- ⁶K. Muraki, S. Fukatsu, Y. Shiraki, and R. Ito, *Appl. Phys. Lett.* **61**, 557 (1992).
- ⁷J. Nagle, J. P. Landesman, M. Larive, C. Mottet, and P. Bois, *J. Cryst. Growth* **127**, 550 (1993).
- ⁸J. F. Zheng, J. D. Walker, M. B. Salmeron, and E. R. Weber, *Phys. Rev. Lett.* **72**, 2414 (1994).
- ⁹H. Yu, C. Roberts, and R. Murray, *Appl. Phys. Lett.* **66**, 2253 (1995).
- ¹⁰S. Martini, A. A. Quivy, E. C. F. da Silva, and J. R. Leite, *Appl. Phys. Lett.* **81**, 2863 (2002).
- ¹¹K. Muraki, S. Fukatsu, Y. Shiraki, and R. Ito, *Surf. Sci.* **267**, 107 (1992).
- ¹²H. Toyoshima, T. Niwa, J. Yamazaki, and A. Okamoto, *Appl. Phys. Lett.* **63**, 821 (1993).
- ¹³Y. C. Kao, F. G. Celii, and H. Y. Liu, *J. Vac. Sci. Technol. B* **11**, 1023 (1993).
- ¹⁴R. Arès, C. A. Tran, and S. P. Watkins, *Appl. Phys. Lett.* **67**, 1576 (1995).
- ¹⁵G. Grenet, E. Bergignat, M. Gendry, M. Lapeyrade, and G. Hollinger, *Surf. Sci.* **352-354**, 734 (1996).
- ¹⁶A. Bosacchi, S. Franchi, P. Pascarella, P. Allegri, and V. Avanzini, *Mater. Sci. Eng., B* **28**, 469 (1994).
- ¹⁷K. Radhakrishnan, S. F. Yoon, R. Gopalakrishnan, and K. L. Tan, *J. Vac. Sci. Technol. A* **12**, 1124 (1994).
- ¹⁸J. P. McCaffrey, Z. R. Wasilewski, M. D. Robertson, and J. M. Corbett, *Philos. Mag. A* **75**, 803 (1997).
- ¹⁹K. Tillmann *et al.*, *Philos. Mag. Lett.* **74**, 309 (1996).
- ²⁰A. Höpner, H. Seitz, I. Rechenberg, F. Bugge, M. Procop, K. Scheersmidt, and H. J. Queisser, *Phys. Status Solidi A* **150**, 427 (1995).
- ²¹P. Yashar, M. R. Pillai, J. Mirecki-Millunchick, and S. A. Barnett, *J. Appl. Phys.* **83**, 2010 (1998).
- ²²S. Martini, A. A. Quivy, M. J. da Silva, T. E. Lamas, E. C. F. da Silva, J. R. Leite, and E. Abramof, *J. Appl. Phys.* **94**, 7050 (2003).
- ²³K. Chattopadhyay, J. Aubel, S. Sundaram, J. E. Ehret, R. Kaspi, and K. R. Evans, *J. Appl. Phys.* **81**, 3601 (1997).
- ²⁴C. Monier, J. Leymarie, A. M. Ceschin, N. Grandjean, A. Vasson, A. M. Vasson, M. Leroux, and J. Massies, *J. Phys. IV* **03**, C5-295 (1993).

- ²⁵M. Zhong, J. Steinshnider, M. Weimer, and R. Kaspi, *J. Vac. Sci. Technol. B* **22**, 1593 (2004).
- ²⁶J. Steinshnider, J. Harper, M. Weimer, C.-H. Lin, S. S. Pei, and D. H. Chow, *Phys. Rev. Lett.* **85**, 4562 (2000).
- ²⁷G. Gonzalez de la Cruz, *J. Appl. Phys.* **96**, 3752 (2004).
- ²⁸M. Schowalter, A. Rosenauer, and D. Gerthsen, *Appl. Phys. Lett.* **88**, 111906 (2006).
- ²⁹M. H. Degani, *Appl. Phys. Lett.* **59**, 57 (1991).
- ³⁰M. Suzuki, *Phys. Lett. A* **146**, 319 (1990).
- ³¹S. A. Chin and C. R. Chen, *J. Chem. Phys.* **114**, 7338 (2001).
- ³²J. M. García, J. P. Silveira, and F. Briones, *Appl. Phys. Lett.* **77**, 409 (2000).
- ³³A. Rosenauer, D. Gerthsen, D. V. Dyck, M. Arzberger, G. Böhm, and G. Abstreiter, *Phys. Rev. B* **64**, 245334 (2001).
- ³⁴J. E. Manzoli, M. A. Romero, and O. Hipólito, *IEEE J. Quantum Electron.* **34**, 2314 (1998).
- ³⁵J. E. Manzoli and O. Hipólito, *Microelectron. Eng.* **43-44**, 221 (1998).
- ³⁶I. H. Tan, G. L. Snider, L. D. Chang, and E. L. Hu, *J. Appl. Phys.* **68**, 4071 (1990).
- ³⁷R. Kaspi and K. R. Evans, *Appl. Phys. Lett.* **67**, 819 (1995).
- ³⁸J. A. Porto and J. Sánchez-Dehesa, *Phys. Rev. B* **51**, 14352 (1995).
- ³⁹L. C. Andreani *et al.*, *J. Appl. Phys.* **78**, 6745 (1995).
- ⁴⁰J. Leymarie, C. Monier, A. Vasson, A.-M. Vasson, M. Leroux, B. Courboulès, N. Grandjean, C. Deparis, and J. Massies, *Phys. Rev. B* **51**, 13274 (1995).
- ⁴¹S. Martini, A. A. Quivy, A. Tabata, and J. R. Leite, *J. Vac. Sci. Technol. B* **18**, 1991 (2000).
- ⁴²C. G. Van de Walle, *Phys. Rev. B* **39**, 1871 (1989).